

20-HETE attenuates the response of glucose-stimulated insulin secretion through the AKT/GSK-3 β /Glut2 pathway

Bijun Zhang^{1,2} · Guangrui Lai¹ · Jingjing Wu² · Ru Sun² · Runhong Xu^{1,2} · Xianghong Yang³ · Yafei Qi³ · Yanyan Zhao^{1,2}

Received: 30 November 2015 / Accepted: 20 June 2016 / Published online: 27 August 2016
© Springer Science+Business Media New York 2016

Abstract We previously generated cytochrome P450 4F2 (*CYP4F2*) transgenic mice that have high levels of 20-hydroxyeicosatetraenoic acid (20-HETE) production; these mice exhibit both hypertension and hyperglycemia without insulin resistance. Currently, it is unclear whether and how 20-HETE affects insulin secretion, thus resulting in hyperglycemia. In this study, we found that 20-HETE attenuated glucose-stimulated insulin secretion (GSIS) in *CYP4F2* transgenic mice as well as in rat insulinoma INS-1E cells treated with 0.5 μ M 20-HETE. HET0016, a selective inhibitor of 20-HETE synthesis, reversed the reduction in GSIS leading to a decrease in blood glucose in the transgenic mice. Furthermore, the expression of glucose transporter 2 (Glut2), Ser⁴⁷³ phosphorylation of protein kinase B (AKT), and Ser⁹ phosphorylation of glycogen synthase kinase-3 β (GSK-3 β) were decreased in *CYP4F2* transgenic mice compared with wild-type mice. In vitro experiments in INS-1E cells revealed that 20-HETE activated the AKT/GSK-3 β pathway and thereby decreased Glut2 expression by inhibiting activator protein 1 (AP-1). TWS119, a GSK-3 β selective inhibitor, blocked the

20-HETE-mediated reduction in Glut2 expression. Therefore, we concluded that 20-HETE inhibition of Glut2 contributes to the reduction in GSIS, at least in part, through the AKT/GSK-3 β /AP-1/Glut2 pathway.

Keywords 20-hydroxyeicosatetraenoic acid · Glucose-stimulated insulin secretion · Glucose transporter 2 · Glycogen synthase kinase-3 β

Introduction

Insulin secretion from pancreatic islet β -cells is regulated by a number of factors; blood glucose is the predominant trigger, while fatty acids and amino acids also act as direct or indirect stimuli [1]. These factors exert some of their effects on insulin secretion via their metabolism in β -cells to generate secretion-coupling signals and raise the ATP/ADP ratio, which serves to suppress ATP-sensitive potassium (K_{ATP}) channels and activate voltage-gated Ca^{2+} channels, leading to insulin granule exocytosis [2]. Glucose-stimulated insulin secretion (GSIS) is central to normal control of metabolic homeostasis and is initiated by glucose uptake into β -cells via the solute carrier family 2 (SLC2A2/Slc2a2, also known as glucose transporter 2 (Glut2)) transporter. Glut2 is a glucose receptor and acts as a first messenger for triggering the glucose signal inside β -cells [3]. Guillam et al. have demonstrated that Glut2-null mice are impaired in glucose signaling resulting in impaired secretion and insulin biosynthesis in β -cells [4]; this secretory defect results only from the absence of the transporter because re-expression of Glut2 by recombinant lentiviruses restores a normal secretory response to glucose [5]. It has been reported that the remarkable reduction in *Glut2*

Electronic supplementary material The online version of this article (doi:10.1007/s12020-016-1031-5) contains supplementary material, which is available to authorized users.

✉ Yanyan Zhao
yyzhao@sj-hospital.org
yyzhao@mail.cmu.edu.cn

- ¹ Department of Clinical Genetics, Shengjing Hospital of China Medical University, Shenyang, Liaoning, China
- ² Department of Medical Genetics, China Medical University, Shenyang, Liaoning, China
- ³ Department of Pathology, Shengjing Hospital of China Medical University, Shenyang, Liaoning, China

expression occurs simultaneously with the loss of GSIS in type 2 diabetic patients [6] and diabetic Chinese hamsters [7]. The expression of Glut2 can be regulated by various kinds of transcription factors including activating protein-1 (AP-1), which can be phosphorylated and negative regulated by glycogen synthase kinase-3 β (GSK-3 β) [8, 9]. In addition to glucose, some fatty acids have been shown either stimulate β -cells directly or potentiate the GSIS response [10]. However, prolonged exposure of β -cells to elevated fatty acids results in impaired insulin secretion by inhibiting insulin biosynthesis [11, 12], promoting apoptosis [13].

Arachidonic acid (AA) is a major membrane fatty acid. Some studies have indicated that glucose stimulation of β -cells is accompanied by release of free AA from glycerolipids and that exogenous AA stimulates an increase in GSIS [14, 15]. AA can be metabolized by cytochrome P450 (CYP) enzymes into eicosanoids, primarily including 20-hydroxyeicosatetraenoic acids (20-HETE) produced by the CYP4A and CYP4F families and epoxyeicosatrienoic acids (EETs) produced by CYP2C and CYP2J families. 20-HETE and EETs exert opposite actions on vascular smooth muscle, inducing vasoconstriction and vasodilatation, respectively [16]. Falck et al. initially reported that EETs stimulate insulin secretion in isolated rat islets [17]. Recently, Luo et al. provided the evidence that genetic deletion and pharmacological inhibition of soluble epoxide hydrolase, which degrades EETs to dihydroxyeicosatrienoic acids, promote insulin secretion in vivo, resulting in the prevention of hyperglycemia in diabetic mice [18]. Nevertheless, less is known about the role of 20-HETE in the regulation of β -cell function and insulin secretion. Some diabetic animal models exhibit alterations in 20-HETE; for example, OVE26 type 1 diabetic mice have increased CYP4A-dependent 20-HETE in glomeruli [19] and streptozotocin-induced type 1 diabetic rats have unexpectedly high levels of 20-HETE in renal microsomes, contributing to the elevation of vascular reactivity [20]. We previously developed *CYP4F2* transgenic (TG) mice that overproduce 20-HETE, which consequently leads to hypertension and hyperglycemia. We further verified that 20-HETE causes hyperglycemia through excessive glycogenolysis, but does not have an effect on peripheral insulin sensitivity (no insulin resistance) [21–23]. Therefore, it remains to be determined whether 20-HETE modulates GSIS so as to result in hyperglycemia in *CYP4F2* TG mice. To address this question, we extended the previous studies in *CYP4F2* TG mice by measuring glucose tolerance and GSIS and by analyzing Glut2 expression and its relevant signaling pathway. Furthermore, we used the rat insulinoma INS-1E cell line as a pancreatic β -cell model to explore a possible mechanism underlying 20-HETE modulation of the GSIS response.

Materials and methods

Experimental animals

The *CYP4F2* TG mice are driven by a truncated kidney androgen-regulated protein promoter, as described in our previous report [21]. Experiments were performed on 12 to 16-week-old male *CYP4F2* TG mice that weighed 24–33 g. TG mice were matched by sex, weight, and age with wild-type (WT) control mice. Mice were fed with standard mouse chow, provided water ad libitum, and bred under a 12 h light/12 h dark cycle system. All experiments conformed to the guide for the care and use of laboratory animals and were approved by the Animal Care Committee of Shengjing Hospital. For 20-HETE inhibition, mice were injected intraperitoneally with either *N*-hydroxy-*N'*-(4-butyl-2 methylphenyl) formamidine (HET0016) (Cayman Chemical Co., Ann Arbor, MI) at 10 μ g/g body weight daily or lecithin (Roche Applied Science, Basel, Switzerland) vehicle (10 % weight per volume lecithin in saline) for 14 days according to the relevant references about HET0016 administration [24, 25].

Cell culture

Rat insulinoma INS-1E cells were cultured in a humidified atmosphere containing 5 % CO₂ in RPMI 1640 medium (HyClone, GE Healthcare, Life Technologies) with 10 mM HEPES, 1 mM sodium pyruvate, 50 μ M 2-mercaptoethanol (Sigma, St. Louis, MO, USA), 100 U/mL penicillin, and 100 μ g/mL streptomycin (HyClone, GE Healthcare, Life Technologies). Once the cells reached 80 % confluence in six well plates, the cells were placed in fetal bovine serum (FBS)-free media for 4 h and then treated with 20-HETE at different concentrations (0.5, 1, 4, or 8 μ M for 1 h; Cayman Chemical), or a selective inhibitor of GSK-3 β 4, 6-disubstituted pyrrolopyrimidine (TWS119, 10 μ M) [26] (Selleck Chemicals, Houston, TX, USA) before the addition of 20-HETE.

Pancreatic 20-HETE analysis

Pancreatic 20-HETE was measured using an API 3200 Q-trap liquid chromatography-tandem mass spectrometry System (LC-MS) (Applied Biosystems, Foster City, CA). Generally, pancreas samples were homogenized in 0.1 % formic acid in methanol, and then 2 ng 20-HETE-d6 (Cayman Chemical) was added as an internal standard. Lipids were extracted with ethyl acetate, dried under nitrogen, and resuspended in methanol. The detection method was carried out as previously described [23]. The effluent was ionized using negative ion electrospray and quantified via multiple reaction monitoring. The ion abundance of 20-HETE in the peaks vs. that of

20-HETE-d6 was determined and compared with standard curves generated over a range from 0.2 to 10 ng.

Glucose tolerance and insulin secretion test

Before performing intraperitoneal glucose tolerance tests (IPGTTs), mice were food-deprived with water overnight. After the mice were weighed, a baseline blood sample was obtained from inner canthus veniplex and additional blood samples were obtained at 30, 60, and 120 min following intraperitoneal injection of glucose at 2.0 mg/g body weight. Plasma glucose and insulin were determined by the oxidase-peroxidase method and a mouse C-peptide ELISA kit (R&D Systems, Minneapolis, MN), respectively.

Measurement of insulin concentration in INS-1E cells

INS-1E cells (1×10^6 cells/well) were seeded in six well plates. Prior to the insulin secretion assay, the cells were starved overnight in Krebs Ringer buffer (135 mM NaCl, 3.6 mM KCl, 1.5 mM CaCl₂, 0.5 mM MgCl₂, 0.5 mM NaH₂PO₄, 5 mM NaHCO₃, and 10 mM HEPES) containing 0.1 % bovine serum albumin (BSA) without glucose and were washed twice with the same buffer. The cells were then incubated in Krebs Ringer buffer with 0.5 μM 20-HETE for 1 h and 16.7 mM glucose for 5, 10, or 60 min. The media was collected and insulin secretion was determined using a rat insulin ELISA kit (R&D Systems, Minneapolis, MN).

Protein extraction

Cytoplasmic and plasma membrane (PM) proteins were extracted using a kit according to the manufacturer's instructions (Beyotime Institute of Technology, Jiangsu, China). Total protein was prepared by homogenizing the frozen tissues or cells in a lysis buffer containing protease and phosphatase inhibitors. Protein concentration was determined using the Bradford method.

Western blot

Denatured protein was separated by electrophoresis and transferred onto polyvinylidene fluoride membranes (Bio-Rad Laboratories, Hercules, CA) at 4 °C. Membranes were subsequently incubated with primary antibody in 5 % BSA at 4 °C overnight followed by horseradish peroxidase-conjugated IgG (ZSGB-BIO, Beijing, China) as the secondary antibody at room temperature for 1 h. The final detection reaction was performed with an ECL detection kit (Beyotime Institute of Technology, Jiangsu, China). The antibodies used for Western blot were as follows: anti-GSK-3β, anti-phospho-GSK-3β, anti-protein kinase B (AKT), and anti-phospho-AKT antibodies (1:1000) (Cell Signaling Technology, Danvers, USA);

anti-Glut2 antibodies (1:500) (Santa Cruz Biotechnology, Santa Cruz, USA); anti-GAPDH antibody (1:10000) (Proteintech Group, Chicago, IL, USA).

Real-time PCR

Total RNA was extracted from the tissues or cells using TRIzol reagent (Invitrogen, Carlsbad, USA) and reverse transcribed into cDNA using a reverse transcription reagent kit (Promega, Madison, USA). Real-time PCR was performed on an ABI 7900 System (Applied Biosystems, Foster City, USA) in a 20 μl SYBR Green PCR reaction containing 1 × SYBR Green PCR master mix (Applied Biosystems, Foster City, USA), 10 ng cDNA and 100 nM forward and reverse primers. The sequences of the primers were 5'-CAATTCATCATCGCCCTCT-3' (forward) and 5'-TGCAGCAATTCGTCAAAG-3' (reverse) for rat *Glut2*; 5'-GTGCCCTGGGTACTCTT-3' (forward) and 5'-TCTTTGCCCTGACTTCCT-3' (reverse) for mouse *Glut2*; and 5'-TGCACCACCAACTGCTTAGC-3' (forward) and 5'-GGCATGGACTGTGGTCATGAG-3' (reverse) for *GAPDH*. Cycle threshold values were analyzed using SDS2.4 software (Applied Biosystems, Foster City, USA).

Plasmid construction

A series of truncated *Glut2* promoter luciferase reporter vectors were constructed. The promoter fragment from -807 to +114 of the *Glut2* gene (GenBank NC_000069) was obtained by PCR using mouse genomic DNA as the template. The p807-Luc, p606-Luc, p337-Luc, and p77-luc constructs were generated with the forward primers 5'-GGGGTACCGGAAGAAACAGGGTCAAG-3' (-807), 5'-GGGGTACCCATCTTGAGATACTGAC-3' (-606), 5'-GGGGTACCACACAGATAACCGATGC-3' (-337), 5'-GGGGTACCATTGGGGTAAAGGGTGT-3' (-77), and with the reverse primer 5'-CCCAAGCTTTGTGTGTGTGTGGAATTGTC-3' containing *KpnI* and *HindIII* sites (underlined), respectively. The amplified product was cloned into the pGL3-basic vector to generate pGlut2-Luc, and all constructs were confirmed to have no coding frame shift in the luciferase gene using sequencing.

Chromatin-immunoprecipitation (ChIP)

INE-1E cells were treated (or not treated) with 20-HETE. ChIP assays were performed as described previously [27]. The lysate was incubated with anti-c-Jun (1:200) (Santa Cruz Biotechnology, Santa Cruz, USA) or nonimmune rabbit IgG (1:200) (Santa Cruz Biotechnology, Santa Cruz, USA) as a negative control at 4 °C overnight. The DNA product was analyzed by PCR with forward primers 5'-GTCTTCCCGACACCAC-3' and reverse primer

5'-TCAATACACCCTTTACCC-3'. The product is a 190 bp fragment of the *Glut2* promoter including the AP-1 binding site. All of the shown data represent the average of at least three independent ChIP experiments.

Transient transfection and luciferase assays

INS-1E cells (5×10^4 cells/well) were subcultured into 24 well plates, grown to 80–90 % confluence after 24 h, and transiently transfected using jetPRIME transfection reagent (Polyplus-transfection, France) with 0.5 μ g of pGlut2-Luc plasmid and 0.01 μ g of pRL-TK encoding for *Renilla* luciferase, which was used to normalize transfection efficiency. After transfection for 6 h, cells were replenished with media containing 0.5 μ M 20-HETE for an additional 18 h. The cells were harvested and the luciferase activities were measured using the Dual-Luciferase Reporter Assay system using a Lumat LB9507 luminometer (Bethold Technologies, Bad Wildbad, Germany).

Immunohistochemistry

Pancreata collected from both WT and TG mice were immediately fixed in 4 % paraformaldehyde, followed by a standard protocol of dehydration and paraffin wax embedding. Pancreatic tissue sections (4 μ m thick) were then prepared and incubated with primary antibodies at room temperature. Using the streptavidin peroxidase-conjugation method, diaminobenzidine (Maxmim Bio-Tech, Fuzhou, China) was utilized as the chromagen to localize peroxidase activity. Photomicrographs were taken with an OLYMPS IX51 inverted microscope with the OLYMPUS Micro software.

Immunofluorescence

INS-1E cells grown on 0.13 mm thick slides were washed with 0.01M (136.9 mM NaCl, 2.68 mM KCl, 8.1 mM $\text{Na}_2\text{HPO}_4 \cdot 12\text{H}_2\text{O}$ and 1.9 mM KH_2PO_4) Phosphate Buffer Saline (PBS), fixed by immersion at room temperature with 4 % polyformaldehyde for 20 min, permeabilized with 0.2 % Triton X-100 in PBS at 4 °C for 10 min, then washed with PBS three times for 5 min. Then the slides were blocked with blocking buffer, consisting of 10 % FBS in PBS, for 30 min at room temperature and incubated with primary antibodies, diluted 1:100 in blocking buffer, overnight at 4 °C. After washing with PBS as before, slides were incubated with a secondary Alexa Fluor®488-Conjugated AffiniPure Goat Anti-Rabbit antibody (ZSGB-BIO, Beijing, China), diluted 1:200 in blocking buffer, at room temperature for 1 h. Subsequently, cells were stained with DAPI for 2 min and washed with PBS. Coverslips and stained cells were captured and analyzed by a confocal laser scanning microscopy system.

Calcium analysis

Cytosolic free calcium was detected using Fluo-3AM. Fluo-3 AM itself does not bind Ca^{2+} , but it is readily hydrolyzed to Fluo-3 AM by endogenous esterases once the dye enters the cell; Fluo-3 AM will emit fluorescence only when it binds to Ca^{2+} . Approximately 1×10^6 cells were harvested and resuspended in 1 ml D-Hank's solution (HyClone, GE Healthcare, Life Technologies) and loaded with Fluo-3AM at a concentration of 1 μ M at 37 °C for 20 min. After washing twice with D-Hank's solution, the resulting fluorescence, an indicator of Ca^{2+} , was monitored using a flow cytometer at excitation wavelength 488 nm.

Statistical analysis

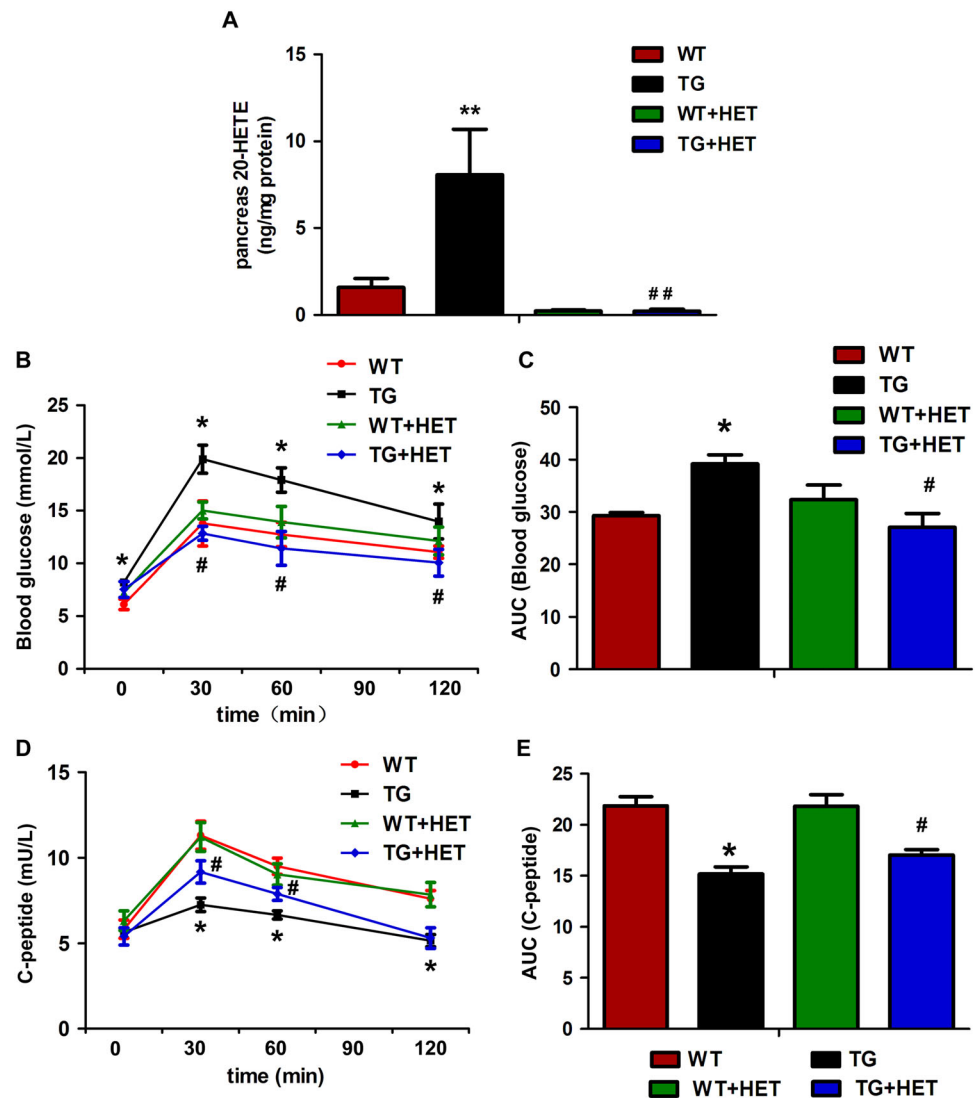
Data were expressed as means \pm SD. All data were analyzed using SPSS v 17.0 software (IBM Corp, Armonk, NY). Student's independent two-tailed test or a one-way ANOVA followed by S-N-K test were used for statistical analysis. Statistical significance was set at $P < 0.05$.

Results

20-HETE impaired glucose tolerance and insulin secretion

First, we detected the pancreatic 20-HETE level in TG mice by LC-MS/MS. As shown in Fig. 1a, the 20-HETE level was higher in TG mice than in WT mice (8.08 ± 2.61 vs. 1.58 ± 0.54 ng/mg protein); an acute lowering of 20-HETE production was detected in both TG (0.25 ± 0.05 ng/mg protein) and WT mice (0.24 ± 0.09 ng/mg protein) after administration of HET0016. To determine the reason for the increased fasting plasma glucose in *CYP4F2* TG mice with 20-HETE overproduction as previously reported, we measured glucose tolerance via IPGTT and insulin secretion by ELISA for plasma levels of C-peptide. After glucose administration, blood glucose was higher in the TG mice than in the WT mice at the indicated time (0 min: 8.22 ± 0.23 vs. 5.36 ± 0.47 mmol/L; 30 min: 19.88 ± 1.33 vs. 13.78 ± 2.13 mmol/L; 60 min: 17.90 ± 1.15 vs. 12.73 ± 1.22 mmol/L; and 120 min: 13.97 ± 1.65 vs. 11.07 ± 0.59 mmol/L, respectively) (Figs. 1a and b). The plasma C-peptide level did not differ at 0 min between the WT control and TG mice (5.83 ± 0.54 vs. 5.66 ± 0.22 mU/L); however, from 30 to 120 min after glucose administration, the plasma C-peptide level was lower in the TG mice than in the WT mice (30 min: 7.26 ± 0.39 vs. 11.32 ± 0.83 mU/L; 60 min 6.66 ± 0.24 vs. 9.51 ± 0.48 mU/L; 120 min: 5.15 ± 0.36 vs. 7.61 ± 0.48 mU/L) (Figs. 1c and d). Furthermore, HET0016, a selective inhibitor of 20-HETE synthesis, was

Fig. 1 20-HETE impairs glucose tolerance and reduced plasma insulin **a** Pancreatic 20-HETE analysis by LC-MS/MS. **b** Intraperitoneal glucose tolerance test (IPGTT) by ELISA. **c** Area under the curve (AUC) derived from blood glucose levels during IPGTT. **d** Detection of plasma C-peptide level by ELISA. **e** AUC derived from plasma C-peptide levels during GSIS in WT mice, *CYP4F2* TG mice, and HET0016 treated groups. Data are presented as mean \pm SD obtained from three independent experiments. $n = 4$ for each group of mice. * $P < 0.05$, ** $P < 0.01$ vs. WT mice; # $P < 0.05$, ## $P < 0.01$ vs. TG mice

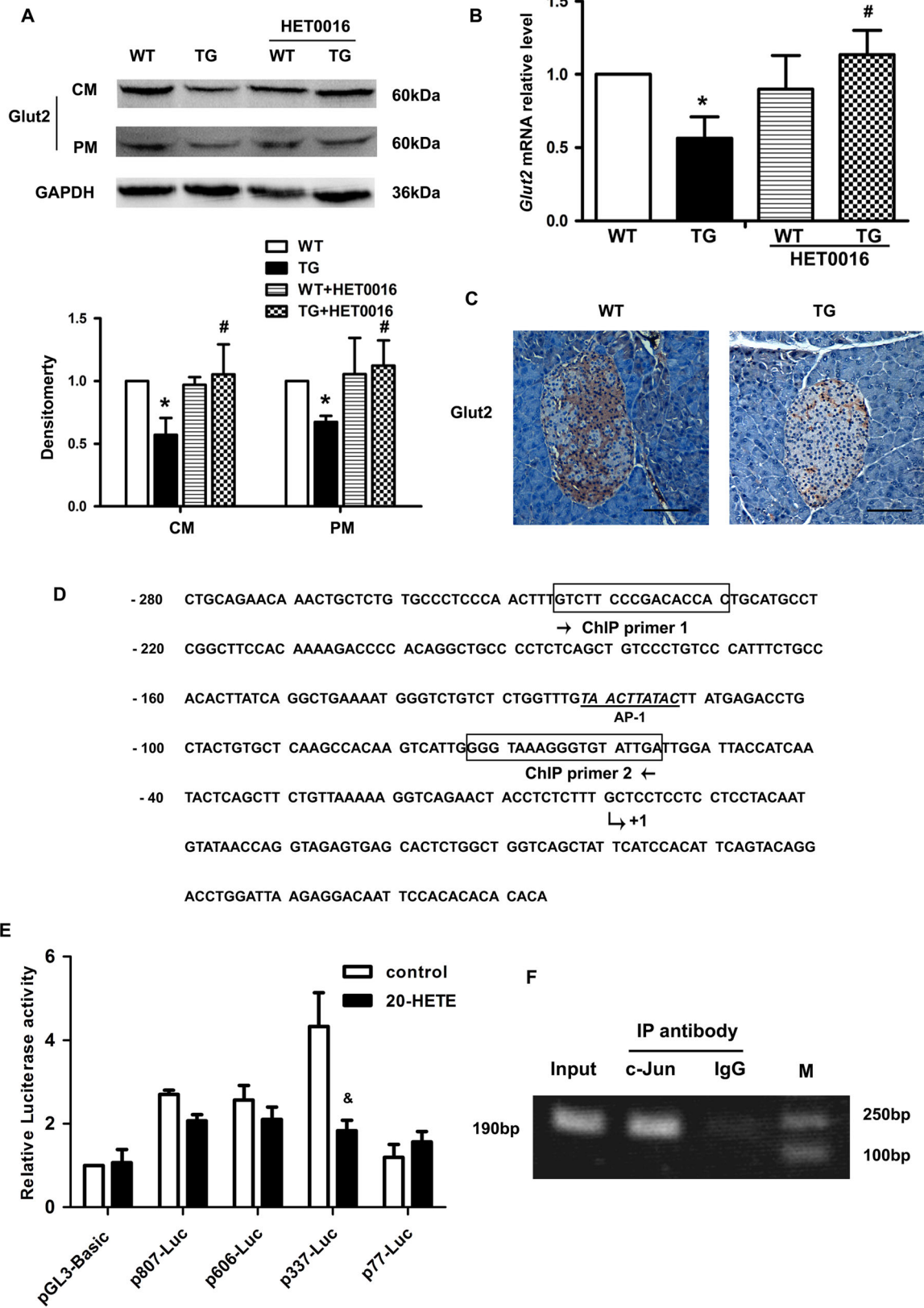


injected into the TG mice for 2 weeks before the IPGTT test. As expected, HET0016 blocked the increase in blood glucose (0 min: 7.55 ± 0.76 mmol/L; 30 min: 12.85 ± 0.66 mmol/L; 60 min: 11.43 ± 1.60 mmol/L; and 120 min: 10.07 ± 1.27 mmol/L) and reversed the reduction in plasma C-peptide (0 min: 5.41 ± 0.50 mU/L; 30 min: 9.18 ± 0.65 mU/L; 60 min: 7.88 ± 0.38 mU/L; and 120 min: 5.31 ± 0.60 mU/L) in the TG mice. These data illustrate that overproduction of 20-HETE causes a dysfunction of insulin secretion and thereby leads to increased plasma glucose in *CYP4F2* TG mice.

20-HETE decreased *Glut2* expression

Since GSIS is initiated by glucose uptake through the *Glut2* transporter, *Glut2* expression was detected in pancreas of mice by Western blot and Real-time PCR. As shown in Figs. 2a and b, protein levels of *Glut2* were decreased in both the cytoplasm (CP) and PM (reduced by 43 and 33 %, respectively) in

pancreatic tissue from TG mice compared with the WT mice, as well as mRNA levels (reduced by 44 %). Furthermore, HET0016 treatment noticeably reversed the reduction in *Glut2*. Immunohistochemistry also confirmed the marked reduction of *Glut2* protein in the islets of TG mice (Fig. 2c). To identify that 20-HETE decreased *Glut2* expression through transcriptional regulation, we constructed a series of truncated *Glut2* promoters and analyzed the 5'-flanking region (-807 to +114) of the mouse *Glut2* gene. As shown in Fig. 2e, we observed that the p337-luc activity was higher than other constructs and was significant reduced after 20-HETE treatment. A putative AP-1 binding motif (TAACCTATAC) was predicted at position -122/-113 (Fig. 2d) and the underlined core sequence resembled the TGACTCA motif found in the consensus AP-1 (c-Jun/c-Fos complex) binding site. In addition, a ChIP assay was carried out in INS-1E cells to confirm that c-Jun was associated with the AP-1 element of the *Glut2* promoter.



◀ **Fig. 2** 20-HETE suppresses the *Glut2* expression by reducing the transcription activity of *Glut2* gene in *CYP4F2* TG mice. **a** CP and PM of *Glut2* expression in WT, TG, and HET0016 treatment group mice. GAPDH was shown as internal control. **b** mRNA levels of *Glut2* in WT, TG, and HET0016 treatment group mice. **c** Immunohistochemical staining for *Glut2* of WT and TG mice. Micrographs were taken at $\times 200$ magnification, and Scale bar = 50 μm . **d** Partial sequence of the 5'-flanking region of the *Glut2* gene. Potential binding site of transcription factor AP-1 was underlined. The locations of the primers used for ChIP are boxed. The transcription initiation site is indicated by a bent arrow and "+1". **e** The *Glut2* promoter activity in INS-1E cells treated with 20-HETE was detected by luciferase assay. Luciferase activities were measured and normalized to Renilla luciferase activities. The fold change of pGL3-basic vector in control group was taken as "1". **f** ChIP assays with c-Jun antibody. Chromatin from INS-1E cells was immunoprecipitated with anti-c-Jun antibody, or nonimmune IgG (negative control). Input was total chromatin DNA used in the PCR reaction as a positive control. M represented DL2000 DNA marker. Data are presented as mean \pm SD obtained from three independent experiments. $n = 4$ for each group of mice. * $P < 0.05$ vs. WT mice; # $P < 0.05$ vs. TG mice; &P < 0.05 vs. control group

The chromatin from INS-1E cells was immunoprecipitated with c-Jun antibody, then we amplified the -245 to -56 region containing the AP-1 element and obtained a 190 bp product. As shown in Fig. 2f, all bindings were specific, as antibody against c-Jun but not nonimmune IgG, immunoprecipitated AP-1 protein bound to the *Glut2* promoter. Therefore, these data demonstrate that 20-HETE is able to reduce *Glut2* expression via transcriptional downregulation.

20-HETE alters phosphorylation of the AKT/GSK-3 β pathway in pancreatic tissue

To address the mechanism underlying 20-HETE downregulated *Glut2* transcription, GSK-3 β was chosen for investigation since GSK-3 β has been implicated not only in the regulation of glucose transport but also in negative regulation of the transcriptional factor, AP-1, by phosphorylation [28, 29]. We assessed the phosphorylation levels of GSK-3 β and AKT in the pancreas of mice by Western blot and Immunohistochemistry. Ser⁴⁷³ phosphorylation of AKT and Ser⁹ phosphorylation of GSK-3 β were both decreased (47 and 49 %) in *CYP4F2* TG mice compared with WT mice and HET0016 treatment eliminated the decrease in GSK-3 β and AKT phosphorylation in TG mice (Figs. 3a and c). Immunohistochemistry also confirmed the marked reduction of the phosphorylation levels of GSK-3 β and AKT in the islets of TG mice (Figs. 3b and d). These data indicate that GSK-3 β is involved in transcriptional regulation of *Glut2* in the pancreas of *CYP4F2* TG mice.

20-HETE modulates the AKT/GSK-3 β pathway in INS-1E cells

To certify that 20-HETE stimulates the AKT/GSK-3 β pathway, we performed in vitro experiments in 20-HETE-treated

INS-1E cells. We first determined the optimal concentration of 20-HETE for treatment in INS-1E cells. Among four concentrations of 20-HETE (0.5, 1, 4, and 8 μM), the 0.5 μM 20-HETE for 1 h treatment led to a 90 % decrease in Ser⁹ phosphorylation of GSK-3 β (Fig. 4a) and also 50 % decrease in Ser⁴⁷³ phosphorylation of AKT (Fig. 4c), indicating the augmented AKT/GSK-3 β activity. These findings were confirmed by immunofluorescence images obtained from INS-1E cells after 20-HETE treatment (Figs. 4b and d). These data illustrate that 20-HETE activates the AKT/GSK-3 β pathway in INS-1E β -cells.

20-HETE downregulated *Glut2* expression and reduced insulin secretion via AKT/GSK-3 β pathway in INS-1E cells

Given that 20-HETE regulates the AKT/GSK-3 β pathway, we wanted to know whether it could alter *Glut2* expression and insulin secretion. We examined the expression of *Glut2* in INS-1E cells with or without 20-HETE treatment. As shown in Fig. 5a, in both the CP and the PM, the *Glut2* protein level was reduced after 20-HETE treatment as was its mRNA level (Fig. 5b), indicating that 20-HETE reduces the expression of *Glut2* in β -cells. Furthermore, we treated INS-1E cells with 0.5 μM 20-HETE and 16.7 mM glucose and measured the intracellular Ca²⁺ using Fluo-3 AM fluorescence and the insulin concentration in the medium at the indicated time. As shown in Figs. 5c and d, as compared with the control group, the mean fluorescence intensity (MFI) of Fluo-3 AM was significantly decreased in the 20-HETE-treated group, which was consistent with the lack of significant difference in insulin levels between the control group and the 20-HETE-treated group in the first 5 min (6.10 ± 0.35 vs. 5.60 ± 0.11 ng/mg protein), while insulin levels were significantly lower in the 20-HETE treatment group than in the control group at 10 min (5.98 ± 0.32 vs. 7.79 ± 0.37 ng/mg protein) and 60 min (6.43 ± 0.27 vs. 8.02 ± 0.24 ng/mg protein). To further identify whether 20-HETE regulated the expression of *Glut2* through activated GSK-3 β , a GSK-3 β selective inhibitor, TWS119, was administrated for 4 h before 20-HETE incubation and was found to reverse the effect of 20-HETE on *Glut2* expression and on intracellular Ca²⁺ levels, which in turn reverses the effects on insulin secretion (10 min: 7.43 ± 0.37 ng/mg protein and 60 min: 7.80 ± 0.51 ng/mg protein) (shown in Figs. 5c and d). Taken together, these findings confirm that 20-HETE can attenuate insulin secretion through the AKT/GSK-3 β /*Glut2* pathway in vitro.

Discussion

In this study, we found that an excess of 20-HETE contributed to a decrease in the GSIS response, combined with

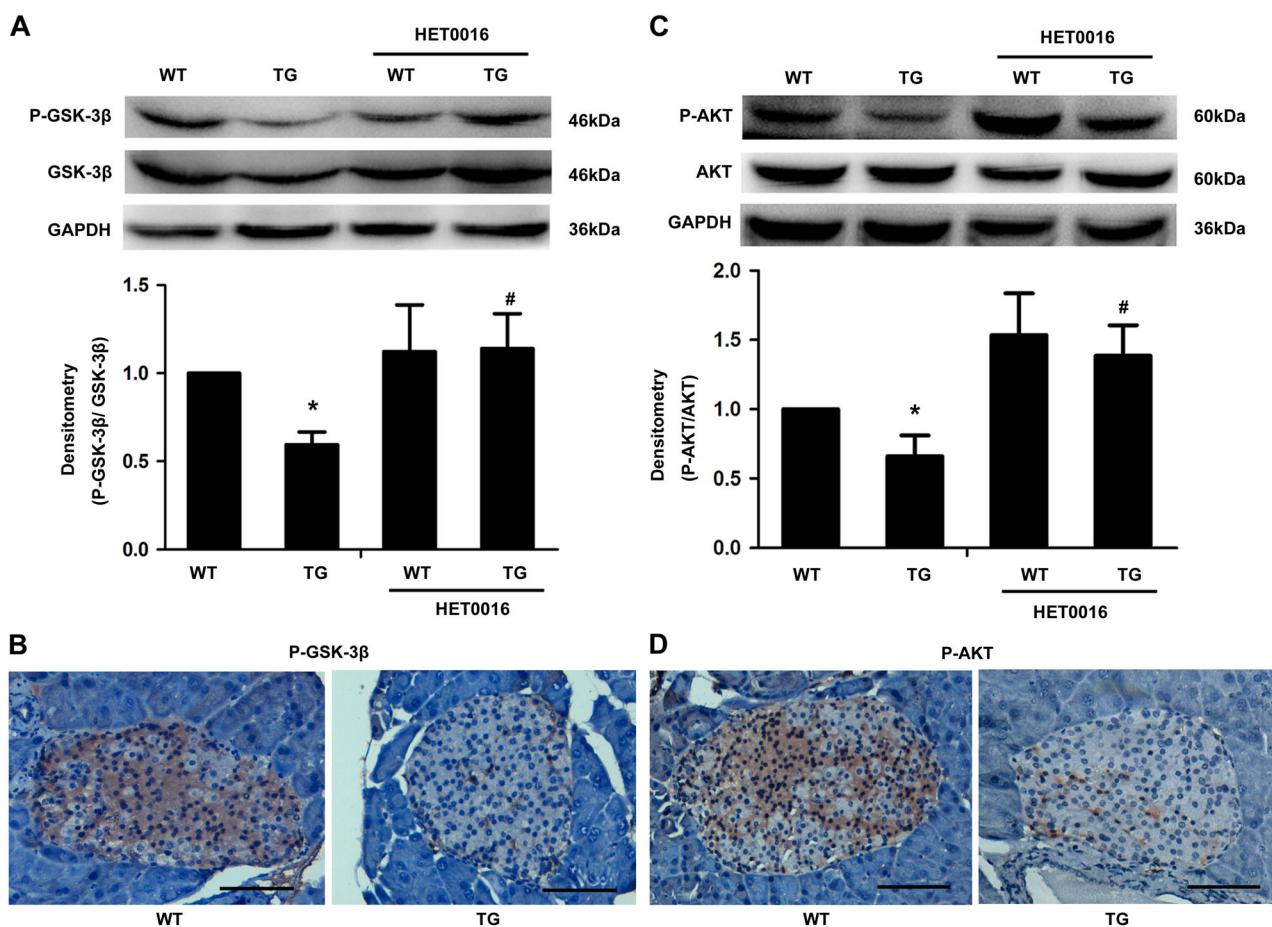


Fig. 3 The phosphorylation levels of AKT and GSK-3 β are reduced in *CYP4F2* TG mice and increased after HET0016 treatment. **a, c** Pancreas P-AKT and P-GSK-3 β expression in WT mice, TG, and HET0016 treatment group mice. Total protein of AKT and GSK-3 and GAPDH were shown as internal control. **b, d** Immunohistochemical staining for

P-AKT and P-GSK-3 β of WT and TG mice. Micrographs were taken at $\times 200$ magnification, and Scale bar = 50 μ m. Data are presented as mean \pm SD obtained from three independent experiments. $n = 4$ for each group of mice. * $P < 0.05$ vs. WT mice; # $P < 0.05$ vs. TG mice

the augmentation of glycogenolysis as reported previously, thereby producing hyperglycemia in *CYP4F2* TG mice. Importantly, we revealed for the first time, both in vivo and in vitro, that 20-HETE could downregulate *Glut2* expression via the AKT/GSK-3 β pathway, which contributes to the pathogenesis of insulin secretion dysfunction.

Most instances of hyperglycemia are associated with pancreatic β -cell function and/or peripheral insulin sensitivity. *CYP4F2* TG mice without insulin resistance allowed us to focus on β -cell dysfunction. So far little research has been devoted to the influence of 20-HETE on β -cell function. Upon initial performance of the glucose tolerance test and GSIS assays, we found that blood glucose levels were significantly elevated in *CYP4F2* TG mice after intraperitoneal injection of glucose. We also observed reduced GSIS, indicating dysfunction of β -cells. A selective inhibitor of 20-HETE synthesis, HET0016, was administered to *CYP4F2* TG mice and significantly improved glucose

tolerance and β -cell function. Moreover, these in vivo results were confirmed in cultured INS-1E cells after with treatment of 20-HETE and high glucose. Therefore, we are the first to demonstrate that 20-HETE participates in the regulation of β -cell function and GSIS.

In rodent pancreatic β -cells, *Glut2*, encoded by the *SLC2A2/Slc2a2* gene, is the major glucose transporter that transports glucose across the PM. GSIS is initiated by glucose taken up by β -cells via *Glut2* and then the glucose enters the mitochondrial respiratory chain where it is metabolized to generate ATP, which results in a Ca^{2+} influx into the CP and finally promotes insulin secretion [2, 3]. One case report described a patient with T2DM that carried a dysfunctional mutation in *SLC2A2* gene, which abolished glucose transport activity [30]. Here, we found that pancreatic *Glut2* expression was decreased in both the CP and the PM in *CYP4F2* TG mice as compared to the WT mice. To confirm the in vivo data, INS-1E cells were treated with

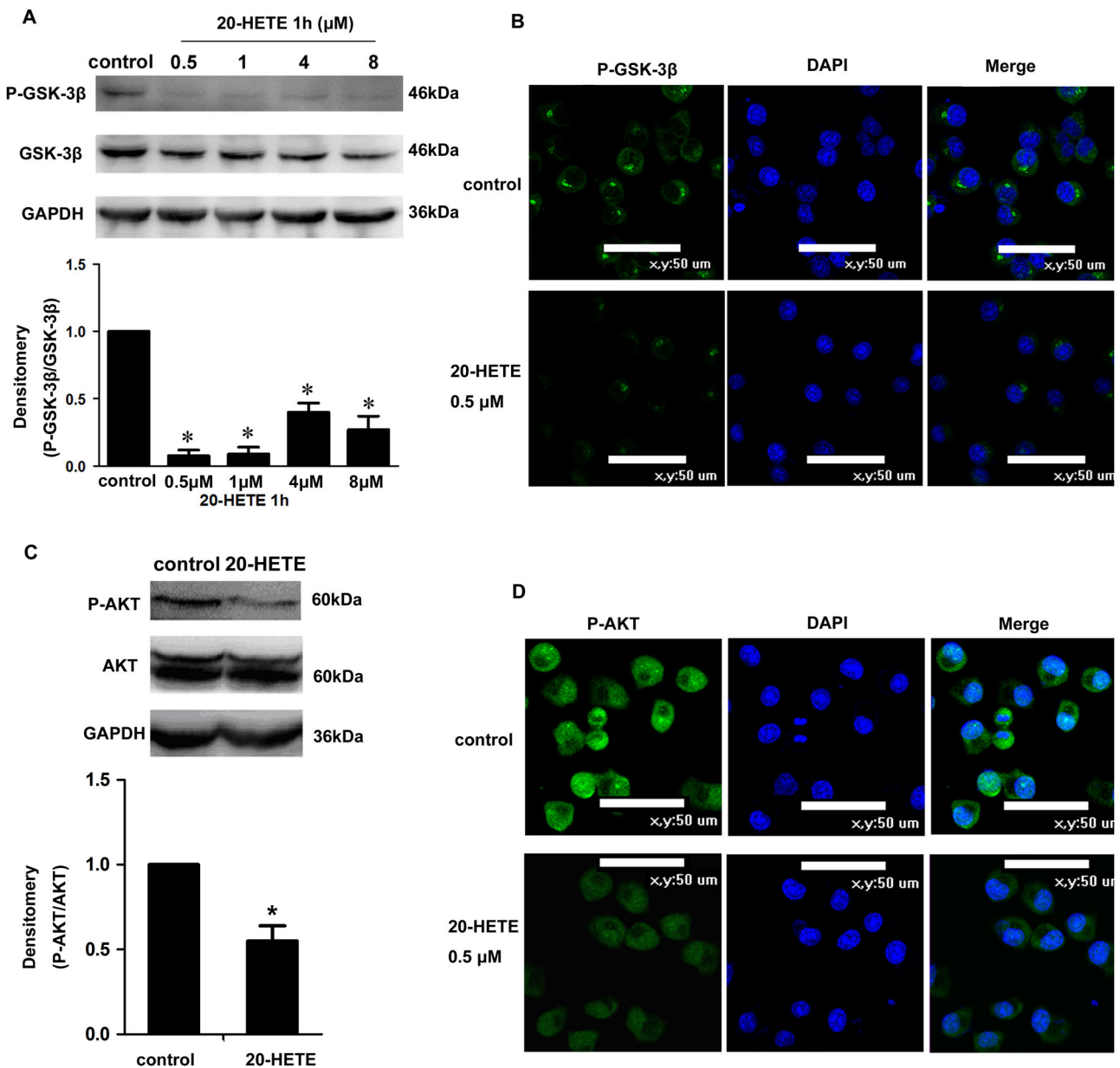


Fig. 4 20-HETE activates the AKT/GSK-3β pathway in INS-1E β-cells. **a** Western blot detected P-GSK-3β expression after different 20-HETE concentration (0.5, 1, 4, and 8 μM for 1 h) treatment in INS-1E β-cells. A concentration of 0.5 μM for 1 h has been used as the optimal condition of 20-HETE treatment, and with this condition, the expression of P-AKT was detected by Western blot, as shown in (c).

Total protein of AKT and GSK-3β and GAPDH were shown as internal control. **b, d** Immunofluorescence analysis: micrographs were taken at a magnification of ×400, and Scale bar = 50 μm. Data are presented as mean ± SD obtained from three independent experiments. **P* < 0.05 vs. control group

20-HETE followed by measurement of *Glut2* mRNA and protein levels. We found that 20-HETE decreased *Glut2* expression by repressing the transcriptional activity of *Slc2a2* gene regulated by the transcriptional factor AP-1. This is the first report that 20-HETE can decrease *Glut2* expression via transcriptional regulation in pancreatic β-cells, which consequently leads to insulin secretion deficiency.

In this study, *CYP4F2* TG mice with hyperglycemia exhibited lower expression of *Glut2*, suggesting that 20-HETE triggers an alternative pathway that leads to regulating *Glut2* transcription. GSK-3 has been implicated in the regulation of glucose transport and metabolism and acts as a negative regulator of basal *Glut1* expression and glucose uptake [28]. GSK-3, as a constitutively active kinase, can be acutely regulated by AKT-mediated phosphorylation at

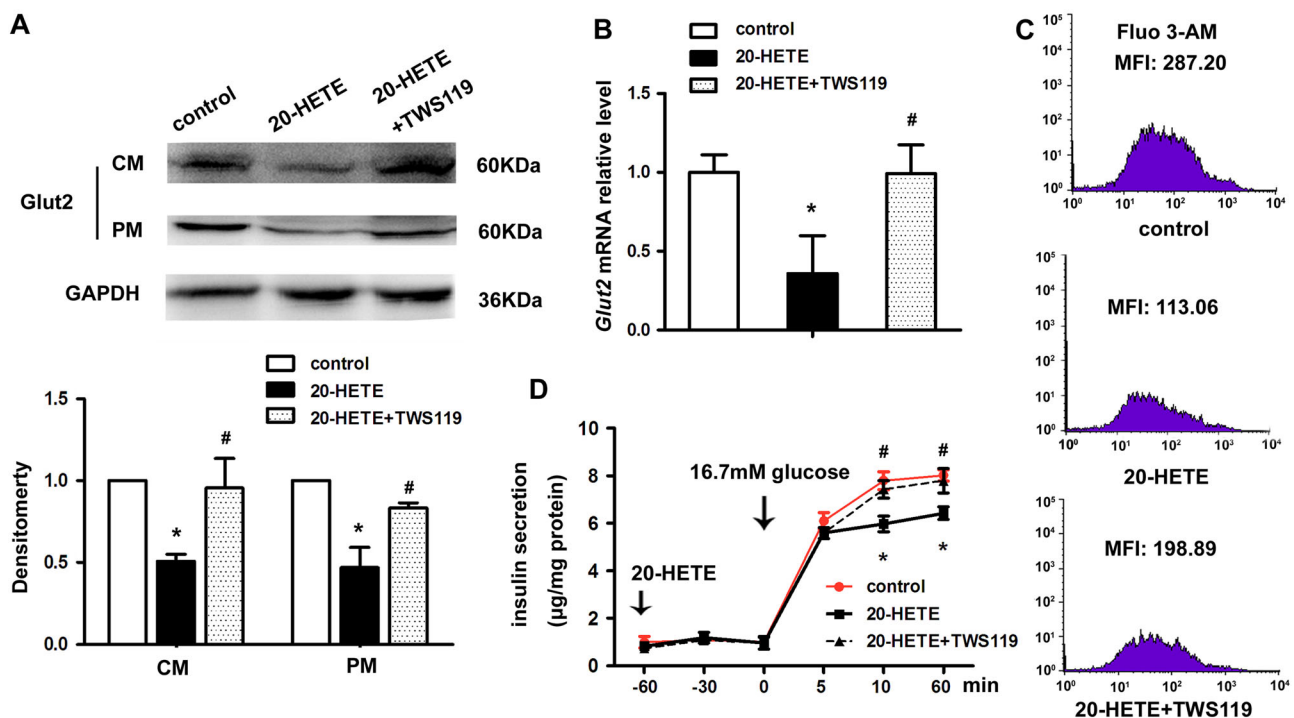


Fig. 5 20-HETE reduces Glut2 expression and inhibits GSIS in INS-1E cells. **a** Western blot detected CP and PM Glut2 expression after 0.5 μ M 20-HETE and the selective GSK-3 β inhibitor TWS119 in INS-1E β -cells. GAPDH was shown as internal control. **b** *Glut2* mRNA expression responded to 20-HETE treatment which was quantified by Real-time PCR. **c** Changes in intracellular Ca²⁺ level of INS-1E cells assayed by flow cytometry. The resulting MFI of

Fluo-3AM was the indicator of intracellular Ca²⁺ levels. **d** Insulin secretion in INS-1E cells. Arrow means to add the 20-HETE 60 min before glucose treatment and 0 min represented the time point for 16.7 mM glucose treatment. Data are presented as mean \pm SD obtained from three independent experiments. * P < 0.05 vs. control group; # P < 0.05 vs. 20-HETE-treated group

Ser²¹ in the α -isoform and Ser⁹ in the β -isoform, leading to a decrease in GSK-3 activity [31]. The two isoforms of GSK-3, GSK-3 α and GSK-3 β , display some important differences regarding their roles in metabolic regulation. Mice with a global knockout of GSK-3 α were viable [32], yet a whole-body knockout of GSK-3 β was lethal [33]; these data suggest that the β -isoform plays a critical role in the development of cells and tissues. It was reported that acute inhibition of the PI3K-PDK1-AKT pathway potentiates insulin secretion [34] and GSK-3 β can phosphorylate and negatively regulate the transcription factor, AP-1 [29, 35, 36]. Therefore, we speculated that 20-HETE can suppress Glut2 via phosphorylation of GSK-3 β . We found that *CYP4F2* TG mice exhibited decreased phosphorylation of AKT and GSK-3 β compared with the WT mice. In addition, in vitro experiments performed in INS-1E cells further confirmed our finding that 20-HETE treatment decreased the phosphorylation of AKT and GSK-3 β as well as reduced Glut2 expression. Furthermore, treatment with TWS119, a selective GSK-3 β inhibitor, reversed the 20-HETE-induced decrease in Glut2 expression at both the mRNA and protein levels. Thus, we concluded

that 20-HETE suppressed Glut2 expression via the AKT/GSK-3 β /AP-1 pathway.

20-HETE is considered to be a potent vasoconstrictor, participating in the regulation of hypertension via the activation of the PKC, MAPK, src-type tyrosine kinase, and the rho kinase pathways [37]. More recently, Ward et al. found that 20-HETE treatment resulted in transient increases in the phosphorylation of AKT in human umbilical vein endothelial cells [38]. By contrast, we reported 20-HETE could decrease the phosphorylation of AKT in the pancreas of *CYP4F2* TG mice as well as in INS-1E cells. An explanation for this phenomenon is that 20-HETE has different effects on different tissues. For example, 20-HETE has been found to decrease cortical blood flow and increase medullary blood flow in kidney [39]. Although no studies have yet shown that elevated 20-HETE production can attenuate insulin secretion, a stable level of EETs can improve stimulated insulin secretion and β -cell function [17]. Our *CYP4F2* TG mice exhibited a disturbed ratio of 20-HETE/EETs and a lower production of EETs overall [40]. According to these data, excess 20-HETE production seems to be the original cause of reduced insulin secretion, acting

at least partially through the AKT/GSK-3 β /AP-1/Glut2 pathway (supplementary Fig. 1).

In summary, multiple experimental approaches and data have identified 20-HETE as an important regulator of hypertension and glucose metabolism. The evidence presented in this study suggests that hyperglycemia induced by 20-HETE in *CYP4F2* TG mice is mediated, in part, via activation of the PI3K/AKT pathway in pancreas. AKT in turn reduces phosphorylation of GSK-3; the consequent activation of GSK-3 results in decreased Glut2 expression levels and decreased glucose uptake. Finally, the reduced Ca²⁺ influx leads to insulin secretion deficiency. Conversely, when the synthesis of 20-HETE is inhibited or GSK-3 β is inactivated, the Glut2 expression level rises, resulting in enhanced insulin secretion. Therefore, we propose that 20-HETE and GSK-3 β may be potential targets for insulin secretion and hyperglycemia therapy.

Acknowledgments This work was supported by a grant from the National Natural Science Foundation of China (Grant No. 81270343) and a grant from the Ministry of Education of China (Grant No. 20122104110020).

Compliance with ethical standards

Conflict of interest The authors declare that they have no conflict of interest.

References

1. C. Tan, U. Voss, S. Svensson, D. Erlinge, B. Olde, High glucose and free fatty acids induce beta cell apoptosis via autocrine effects of ADP acting on the P2Y(13) receptor. *Purinergic Signal*. **9**, 67–79 (2013)
2. M.V. Jensen, J.W. Joseph, S.M. Ronnebaum, S.C. Burgess, A.D. Sherry, C.B. Newgard, Metabolic cycling in control of glucose-stimulated insulin secretion. *Am. J. Physiol. Endocrinol. Metab.* **295**, E1287–E1297 (2008)
3. A. Leturque, E. Brot-Laroche, M. Le Gall, GLUT2 mutations, translocation, and receptor function in diet sugar managing. *Am. J. Physiol. Endocrinol. Metab.* **296**, E985–E992 (2009)
4. M.T. Guillam, E. Hümmler, E. Schaerer, J.I. Yeh, M.J. Birnbaum, F. Beermann et al., Early diabetes and abnormal postnatal pancreatic islet development in mice lacking Glut-2. *Nat. Genet.* **17**, 327–330 (1997)
5. M.T. Guillam, P. Dupraz, B. Thorens, Glucose uptake, utilization, and signaling in GLUT2-null islets. *Diabetes* **49**, 1485–1491 (2000)
6. K. Ohtsubo, M.Z. Chen, J.M. Olefsky, J.D. Marth, Pathway to diabetes through attenuation of pancreatic beta cell glycosylation and glucose transport. *Nat. Med.* **17**, 1067–1075 (2011)
7. A. Jörns, M. Tiedge, E. Sickel, S. Lenzen, Loss of GLUT2 glucose transporter expression in pancreatic beta cells from diabetic Chinese hamsters. *Virchows Arch.* **428**, 177–185 (1996)
8. D.A. Babu, T.G. Deering, R.G. Mirmira, A feat of metabolic proportions: Pdx1 orchestrates islet development and function in the maintenance of glucose homeostasis. *Mol. Genet. Metab.* **92**, 43–55 (2007)
9. J.W. Kim, Y.H. Ahn, C/EBP binding activity to site F of the rat GLUT2 glucose transporter gene promoter is attenuated by c-Jun in vitro. *Exp. Mol. Med.* **34**, 379–384 (2002)
10. S. Schnell, M. Schaefer, C. Schöfl, Free fatty acids increase cytosolic free calcium and stimulate insulin secretion from beta-cells through activation of GPR40. *Mol. Cell Endocrinol.* **263**, 173–180 (2007)
11. S. Kashyap, R. Belfort, A. Gastaldelli, T. Pratipanawatr, R. Berria, W. Pratipanawatr et al., A sustained increase in plasma free fatty acids impairs insulin secretion in nondiabetic subjects genetically predisposed to develop type 2 diabetes. *Diabetes* **52**, 2461–2474 (2003)
12. D.K. Hagman, M.G. Latour, S.K. Chakrabarti, G. Fontes, J. Amyot, C. Tremblay et al., Cyclical and alternating infusions of glucose and intralipid in rats inhibit insulin gene expression and Pdx-1 binding in islets. *Diabetes* **57**, 424–431 (2008)
13. K.S. Gwiazda, T.L. Yang, Y. Lin, J.D. Johnson, Effects of palmitate on ER and cytosolic Ca²⁺ homeostasis in β -cells. *Am. J. Physiol. Endocrinol. Metab.* **296**, E690–E701 (2009)
14. R.N. Bone, Y. Gai, V. Magrioti, M.G. Kokotou, T. Ali, X. Lei et al., Inhibition of Ca²⁺-independent phospholipase A2 β (iPLA2 β) ameliorates islet infiltration and incidence of diabetes in NOD mice. *Diabetes* **64**, 541–554 (2015)
15. G. Dixon, J. Nolan, N.H. McClenaghan, P.R. Flatt, P. News-holme, Arachidonic acid, palmitic acid and glucose are important for the modulation of clonal pancreatic beta-cell insulin secretion, growth and functional integrity. *Clin. Sci. (Lond.)* **106**, 191–199 (2004)
16. R.J. Roman, P-450 metabolites of arachidonic acid in the control of cardiovascular function. *Physiol. Rev.* **82**, 131–185 (2002)
17. J.R. Falck, S. Manna, J. Moltz, N. Chacos, J. Capdevila, Epoxyeicosatrienoic acids stimulate glucagon and insulin release from isolated rat pancreatic islets. *Biochem. Biophys. Res. Commun.* **114**, 743–749 (1983)
18. P. Luo, H.H. Chang, Y. Zhou, S. Zhang, S.H. Hwang, C. Morisseau et al., Inhibition or deletion of soluble epoxide hydrolase prevents hyperglycemia, promotes insulin secretion, and reduces islet apoptosis. *J. Pharmacol. Exp. Ther.* **334**, 430–438 (2010)
19. A.A. Eid, Y. Gorin, B.M. Fagg, R. Maalouf, J.L. Barnes, K. Block et al., Mechanisms of podocyte injury in diabetes: role of cytochrome P450 and NADPH oxidases. *Diabetes* **58**, 1201–1211 (2009)
20. M.H. Yousif, I.F. Benter, K.M. Dunn, A.J. Dahly-Vernon, S. Akhtar, R.J. Roman, Role of 20-hydroxyeicosatetraenoic acid in altering vascular reactivity in diabetes. *Auton. Autacoid Pharmacol.* **29**, 1–12 (2009)
21. X. Liu, Y. Zhao, L. Wang, X. Yang, Z. Zheng, Y. Zhang et al., Overexpression of cytochrome P450 4F2 in mice increases 20-hydroxyeicosatetraenoic acid production and arterial blood pressure. *Kidney Int.* **75**, 1288–1296 (2009)
22. J. Wu, X. Liu, G. Lai, X. Yang, L. Wang, Y. Zhao, Synergistical effect of 20-HETE and high salt on NKCC2 protein and blood pressure via ubiquitin-proteasome pathway. *Hum. Genet.* **132**, 179–187 (2013)
23. G. Lai, J. Wu, X. Liu, Y. Zhao, 20-HETE induces hyperglycemia through the cAMP/PKA-PhK-GP pathway. *Mol. Endocrinol.* **26**, 1907–1916 (2012)
24. F. Park, W.E. Sweeney, G. Jia, R.J. Roman, E.D. Avner, 20-HETE mediates proliferation of renal epithelial cells in polycystic kidney disease. *J. Am. Soc. Nephrol.* **19**, 1929–1939 (2008)
25. J. Cheng, J.S. Ou, H. Singh, J.R. Falck, D. Narsimhaswamy, K.A. Pritchard Jr., M.L. Schwartzman, 20-hydroxyeicosatetraenoic acid causes endothelial dysfunction via eNOS uncoupling. *Am. J. Physiol. Heart Circ. Physiol.* **294**, H1018–H1026 (2008)

26. W. Liu, J. Hao, L. Zhu, F. Li, Q. Liu, S. Liu, S. Zhao, H. Li, H. Duan, Phospho-GSK-3 β is involved in the high-glucose-mediated lipid deposition in renal tubular cells in diabetes. *Int. J. Biochem. Cell Biol.* **45**, 2066–2075 (2013)
27. Y. Zhang, C. Li, W. Li, Y. Zhao, Estrogen regulation of human with-no-lysine (K) kinase-4 gene expression involves AP-1 transcription factor. *Mol. Cell Endocrinol.* **332**, 140–148 (2011)
28. C.L. Buller, R.D. Loberg, M.H. Fan, Q. Zhu, J.L. Park, E. Vesely et al., A GSK-3/TSC2/mTOR pathway regulates glucose uptake and GLUT1 glucose transporter expression. *Am. J. Physiol. Cell Physiol.* **295**, C836–C843 (2008)
29. W.J. Boyle, T. Smeal, L.H. Defize, P. Angel, J.R. Woodgett, M. Karin et al., Activation of protein kinase C decreases phosphorylation of c-Jun at sites that negatively regulate its DNA-binding activity. *Cell* **64**, 573–584 (1991)
30. A. Michau, G. Guillemain, A. Grosfeld, S. Vuillaumier-Barrot, T. Grand, M. Keck et al., Mutations in SLC2A2 gene reveal hGLUT2 function in pancreatic β cell development. *J. Biol. Chem.* **288**, 31080–31092 (2013)
31. J. Jiang, Z.H. Wang, M. Qu, D. Gao, X.P. Liu, L.Q. Zhu, J.Z. Wang, Stimulation of EphB2 attenuates tau phosphorylation through PI3K/Akt-mediated inactivation of glycogen synthase kinase-3 β . *Sci. Rep.* **29**, 11765 (2015)
32. N.J. Pearce, J.R. Arch, J.C. Clapham, M.P. Coghlan, S.L. Corcoran, C.A. Lister et al., Development of glucose intolerance in male transgenic mice overexpressing human glycogen synthase kinase-3 on a muscle-specific promoter. *Metabolism* **53**, 1322–1330 (2004)
33. K.P. Hoefflich, J. Luo, E.A. Rubie, M.S. Tsao, O. Jin, J.R. Woodgett, Requirement for glycogen synthase kinase 3 β in cell survival and NF-kappaB activation. *Nature* **406**, 86–90 (2000)
34. K. Aoyagi, M. Ohara-Imaizumi, C. Nishiwaki, Y. Nakamichi, K. Ueki, T. Kadowaki et al., Acute inhibition of PI3K-PDK1-Akt pathway potentiates insulin secretion through upregulation of newcomer granule fusions in pancreatic β -cells. *PLoS One* **7**, e47381 (2012)
35. J.C. Bournat, A.M. Brown, A.P. Soler, Wnt-1 dependent activation of the survival factor NF-kappaB in PC12 cells. *J. Neurosci. Res.* **61**, 21–32 (2000)
36. J.L. Larabee, F.J. Maldonado-Arocho, S. Pacheco, B. France, K. DeGiusti, S.M. Shakir et al., Glycogen synthase kinase 3 activation is important for anthrax edema toxin-induced dendritic cell maturation and anthrax toxin receptor 2 expression in macrophages. *Infect. Immun.* **79**, 3302–3308 (2011)
37. J.M. Williams, S. Murphy, M. Burke, R.J. Roman, 20-HETE: a new target for the treatment of hypertension. *J. Cardiovasc. Pharmacol.* **56**, 336–344 (2010)
38. N.C. Ward, K. Chen, C. Li, K.D. Croft, J.F. Keaney Jr., Chronic AMPK activation prevents 20-HETE induced endothelial dysfunction. *Clin. Exp. Pharmacol. Physiol.* **38**, 328–333 (2011)
39. A.O. Oyekan, Differential effects of 20-hydroxyeicosatetraenoic acid on intrarenal blood flow in the rat. *J. Pharmacol. Exp. Ther.* **313**, 1289–1295 (2005)
40. X. Liu, J. Wu, H. Liu, G. Lai, Y. Zhao, Disturbed ratio of renal 20-HETE/EETs is involved in androgen-induced hypertension in cytochrome P450 4F2 transgenic mice. *Gene* **505**, 352–359 (2012)